IOP Publishing Journal of Physics: Condensed Matter
J. Phys.: Condens. Matter **27** (2015) 154201 (10pp) doi:10.1088/0953-8984/27/15/154201

Topical Review

Bistable Si dopants in the GaAs (1 1 0) surface

E P Smakman and P M Koenraad

Department of Applied Physics, Eindhoven University of Technology, 5612 AZ Eindhoven, The Netherlands

E-mail: e.p.smakman@tue.nl

Received 30 July 2014, revised 8 September 2014
Accepted for publication 11 September 2014
Published 18 March 2015

Abstract

In this review, recent work is discussed on bistable Si dopants in the GaAs (1 1 0) surface, studied by scanning tunneling microscopy (STM). The bistability arises because the dopant atom can switch between a positive and a negative charge state, which are associated with two different lattice configurations. Manipulation of the Si atom charge configuration is achieved by tuning the local band bending with the STM tip. Furthermore, illuminating the sample with a laser also influences the charge state, allowing the operation of the dopant atom as an optical switch. The switching dynamics without illumination is investigated in detail as a function of temperature, lateral tip position, and applied tunneling conditions. A physical model is presented that independently describes the thermal and quantum tunneling contributions to the switching frequency and charge state occupation of a single Si atom. The basic functionality of a memory cell is demonstrated employing a single bistable Si dopant as the active element, using the STM tip as a gate to write and read the information.

Keywords: dopant, STM, semiconductor

(Some figures may appear in colour only in the online journal)

1. Introduction

Dopants play an important role in the conductivity of semiconductor materials. Commercial electronic devices are shrinking, following Moore's Law [1], with smallest feature sizes currently approaching 10 nm. This means that the dimensions of, for instance, transistors and memory cells are reaching the domain where the local properties of individual dopant atoms start to influence the functionality of the devices. A possible next step in development is the implementation of single dopants as the active elements of operation, resulting in 'solotronic' devices [2]. Recently, various systems have been demonstrated with scanning tunneling microscopy (STM) in which chains of atoms on a surface [3, 4] or dangling bonds at the surface [5, 6] exhibit memory functionality. Other experimental examples of solotronic devices are single atom transistors, where single dopants embedded in a host material act as the active functional element [7, 8]. The bistable Si atom in the GaAs (1 1 0) surface presented in this work switches between a negative and positive charge state, which is associated with a bond reconfiguration. This system was manipulated by the STM tip and by means of laser illumination. Furthermore, dopant bistability was used to demonstrate memory operations, where the STM tip was used to set the charge state to either negative or positive and to subsequently detect the configuration without disturbing it, using separate tunneling conditions.

The measurements discussed here were performed in an Omicron LT-STM on (1 1 0) surfaces of GaAs wafers doped with $\sim 2 \times 10^{18}\,\mathrm{cm}^{-3}$ Si. The tips were made from polycrystalline W wires that were electrochemically etched and further prepared under ultra-high vacuum (UHV) conditions [9].

The Si dopant in GaAs can occupy the Ga or As lattice site and, for sufficiently high doping concentrations, both species form during the material growth. Studies with STM have uncovered the properties of the Si donor at the Ga site [11, 12] and the Si acceptor at the As site [13, 14] near the (1 1 0) surface. The exact depth of the Si dopants is determined from a statistical analysis of the topographic height contrast visible

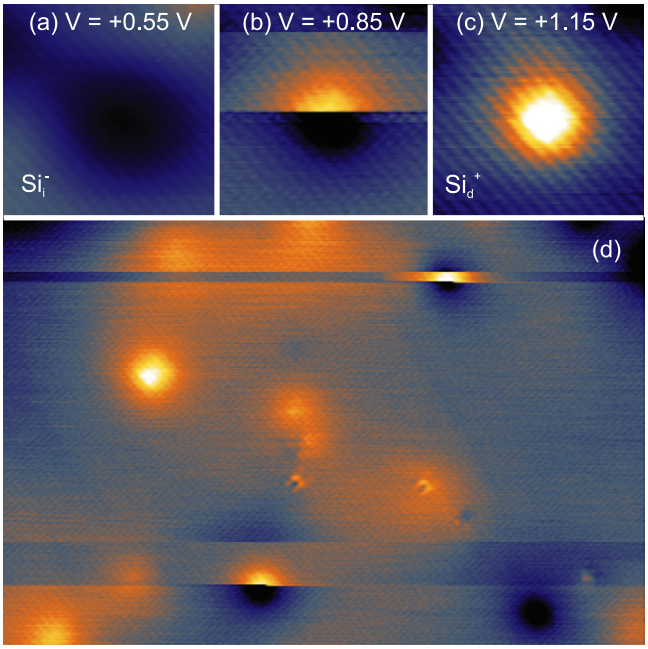

Figure 1. STM topography images demonstrating the bistability of Si in the (1 1 0) surface layer of GaAs. (*a*)–(*c*) $10 \times 10\,\mathrm{nm}^2$ topographic maps taken at $I = 100\,\mathrm{pA}$ representing (*a*) Si_i^-, (*b*) switching behavior, and (*c*) Si_d^+. (*d*) $48 \times 36\,\mathrm{nm}^2$ topographic map revealing Si dopants in and below the surface. Si_a acceptors appear with a dark contrast, Si_d donors appear with a bright contrast, and bistable $\mathrm{Si}_{i,d}$ dopants in the surface layer switch during scanning with the tip. The fast scan direction is left to right, and the slow scan direction is bottom to top, $V = +0.75\,\mathrm{V}$, $I = 50\,\mathrm{pA}$, $T = 5\,\mathrm{K}$. Reprinted with permission from [10]. Copyright 2013 by the American Physical Society.

in the STM topography. The dopant contrast decreases for Si further below the surface. Furthermore, in the case of, for instance, the Si donor, the odd layers are centered on the Ga site at the surface, while the even layers are centered on the As site at the surface. Bistable charge switching of Si dopants in the surface layer of GaAs (1 1 0) was recently observed with STM [10, 15, 16], see figure 1. All and only the Si in the surface layer are bistable. During the scanning of the tip, switching between a dark and a bright contrast appears in the STM images, which correspond to the Coulomb fields of a single negative and positive charge, respectively. When a relatively low bias voltage is applied, the Si is primarily found in the negative charge state Si_i^- and appears dark in the STM topography. For a relatively high bias voltage, the positive charge state Si_d^+ is predominant and the dopant has a bright contrast in the STM images. The stochastic switching between the two charge states occurs during scanning of the tip, when the bias voltage is set to a critical value.

Switching of the charge state corresponds to a change of the exact lattice position of the Si dopant in the surface, summarized in figure 2. In the case of Si_d^+, the atom acts as a substitutional ionized donor and occupies the position of the Ga atom it replaces in the lattice, which is slightly relaxed inwards due to the buckling at the surface. The ionization of the Si donor occurs through the local presence of the STM tip, because of tip induced band bending (TIBB). The bands of the semiconductor bend upwards at positive bias voltage, allowing the weakly bound electron to escape the neutral donor, resulting in Si_d^+. The ionization process is visible in the STM images in the form of a bright disk centered around the Si donor that marks the distance at which the tip must be to pull up the bands enough for the electron to escape [17]. Near the surface, the electron binding energy gradually increases to ∼40 meV [18], which is different from the bulk value of 6 meV. DFT calculations predict that, at the surface, an additional metastable charge state exists, Si_i^-, which relaxes outwards with respect to the surface [19, 20]. The energy state related to this configuration is positioned much deeper into the bandgap, estimated at ∼500 meV.

The bistable Si dopant in the GaAs (1 1 0) surface bears many similarities to the DX^- center in bulk semiconductors, for instance, in the form of the Si dopant in AlGaAs [21, 22]. The DX^- center is a trap for charge carriers, with an energy level located deep in the bandgap. It is created when one of the valence bonds between the Si donor and the neighboring As breaks and the dopant relaxes to an interstitial position in the lattice. When the Si atom sits at the surface, the fourth valence bond does not exist, but the surface relaxation can still take place. In this case, the Si dopant moves outwards with respect to the surface and can accept an additional electron, making it negatively charged [20]. This configuration is energetically the most favorable. The lattice coordinate diagram for the bistable Si atom is displayed in figure 3. The diagram illustrates the total energy of the various charge states as a function of the Si lattice position. Besides the positive and negative charge states two neutral configurations are also indicated. One neutral configuration is located roughly at the position of the relaxed Ga atom the Si dopant replaces. The other neutral configuration resembles the DX^--like situation, with an associated energy in the conduction band. The switching between the positive and neutral charge state at the donor location is considered an electrostatic process, occurring faster than the sample frequency of the STM when feedback is on, which is in the order of 1 ms. Switching to the other DX^--like lattice configuration is expected to involve inelastic processes and is thus generally slow, in the order of seconds at $T = 5\,\mathrm{K}$.

To study the dynamical processes involved in the switching of the Si atom, it is useful to perform an analysis of the random telegraph noise recorded on single bistable dopants. From this analysis, the switching frequency, charge state occupations, and charge state residence times can be extracted. In figure 4, the relative tip-sample distance is displayed, recorded on top of a single bistable Si dopant for three different bias voltages. In these measurements, the tip was restricted to a single point in constant current mode and the height was recorded in time. At a relatively low bias voltage, Si_i^- is stable. Si_d^+ is favored at a relatively high bias voltage. Around the critical voltage where the switching occurs most often, a random telegraph noise signal appears, where the two distinct low and high Z-levels correspond to the negative and positive charge states, respectively. The height difference between the two Z-levels is in the order of 50 pm, which is an order of magnitude larger than the noise level of the STM. At $T = 5\,\mathrm{K}$, the lateral drift of the tip is limited, which allows the

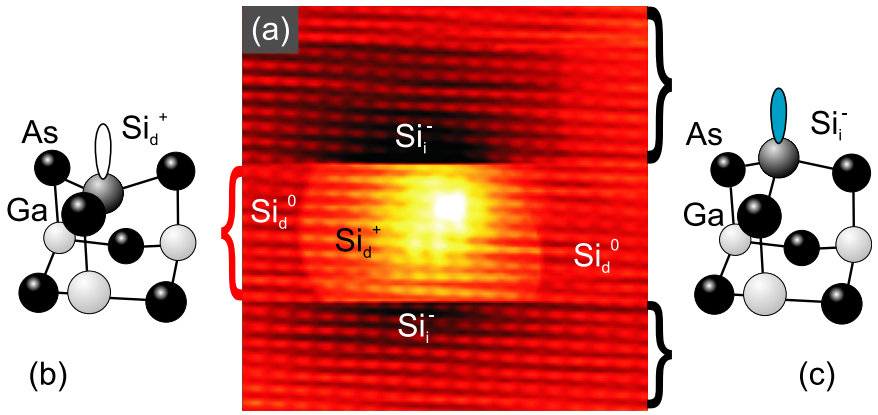

Figure 2. (*a*) $11 \times 9\,\text{nm}^2$ STM topography of a switching Si atom. The fast scan direction is left to right and the slow scan direction is bottom to top, $V = +0.50\,\text{V}$, $I = 500\,\text{nA}$, $T = 5\,\text{K}$. (*b*) Illustration of the positive charge state with an empty dangling bond, relaxed inwards with respect to the surface. (*c*) Illustration of the negative charge state with a filled dangling bond, relaxed outwards with respect to the surface. Adapted with permission from [15]. Copyright 2011 by the American Physical Society.

detailed study of the switching behavior of a single Si atom for measurements taking up to several hours.

To determine if the switching is a fully random process, histograms with the residence times of Si_i^- and Si_d^+ are displayed on a semi-logarithmic scale in figure 5. The data is fitted to a Poissonian distribution [23]:

$$P(t) = \frac{N}{2} p(1-p)^t, \tag{1}$$

where p is the probability to switch to the other state, N is the number of switching events, and t is the time. From the straight fits, we can conclude that the switching follows Poissonian behavior and is thus a random process. p can be expressed as an average switching probability per data point, which are recorded every 1 ms. In this case, for Si_i^-, $p = 0.052 \pm 0.001$ and for Si_d^+, $p = 0.040 \pm 0.002$. Both values are close to each other because the tunneling conditions were set to the critical bias voltage, where escape and capture of electrons occur at roughly the same rate.

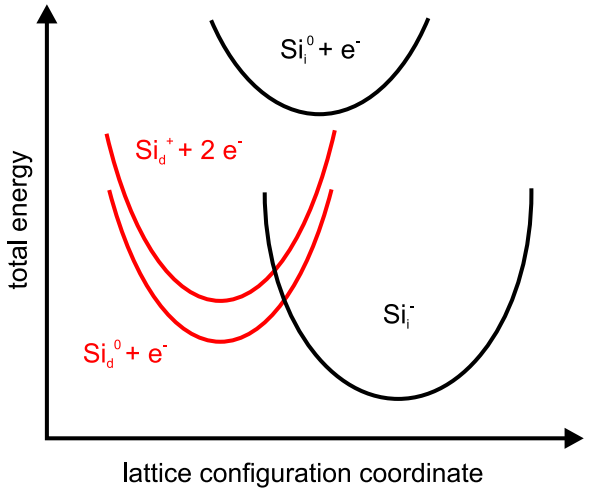

Figure 3. A configuration coordinate diagram of the total energy of the different charge configurations of a bistable Si atom. The extra electrons are included to keep the total charge the same for each configuration. Adapted with permission from [10]. Copyright 2013 by the American Physical Society.

2. Laser and voltage manipulation

The macroscopic illumination of the sample provides an independent method to study the bistable behavior of Si dopants in GaAs (1 1 0) because the absorbed photons create electron-hole pairs that interact with the bistable Si dopant in the surface. The combination of manipulation with laser illumination and detection of the effect with the STM tip comprises a technique that allows us to study the electron capture and escape processes on the Si atom.

To study the optical response of bistable Si dopants, a $\lambda = 632\,\text{nm}$ diode laser was employed to illuminate the sample and tip [10]. A spot size of $\sim$0.1 mm was obtained with a vacuum-build-in lens to focus the light coming from outside the chamber [24]. The laser was repetitively turned on and off while the STM tip scanned over a single 60 nm-wide line, with a bistable Si in the center (see figure 6(*a*)). The 2 nm of the topography directly on top of the Si is displayed, showing the clear switching between the dark and bright contrast in time, corresponding to negative and positive charges, respectively. To cancel out any effects on the topography from the illumination, the GaAs surrounding the dopant was used to level the Si contrast appropriately. When the laser is off, the chosen bias voltage of $V = +0.50\,\text{V}$ favors the negative charge state and no switching is observed in this case. When the laser is on, the dopant atom switches to the positive charge state. The Si atom sometimes switches back to Si_i^-, but this is again followed by a quick ionization. In (*b*), the same type of experimental results are depicted, but for varying laser power P. A clear effect is observed in this case: for higher laser powers, the occupation of Si_d^+ becomes larger. This suggests that the absorbed photons in the semiconductor only play a role in the escape of electrons from the bistable Si atom and not in the capture process.

The relevant processes in the illumination experiments are summarized in figure 7. When the laser is off and the bias voltage is low, shown in (*a*), the electrons are bound to the Si and the negative charge state is predominant. The electrons

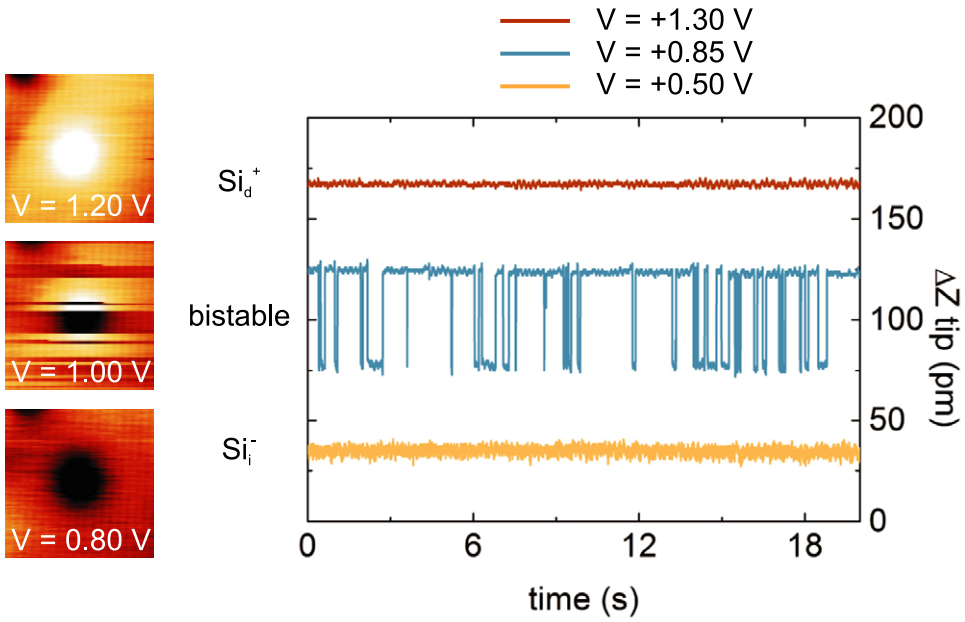

Figure 4. Relative tip-sample distances recorded in time measured with an STM tip restricted directly on top of a single Si dopant. A relatively low bias voltage favors the occupation of Si_i^- and a relatively high bias voltage results in a stable Si_d^+. At the critical voltage, switching occurs between the two charge states, which appears as random telegraph noise in the measurement. $I = 75$ pA, $T = 77$ K. On the left, 8×8 nm^2 STM topographic images are displayed corresponding to the three different situations. $I = 70$ pA, $T = 5$ K. Reprinted with permission from [16]. Copyright 2014 by the American Physical Society.

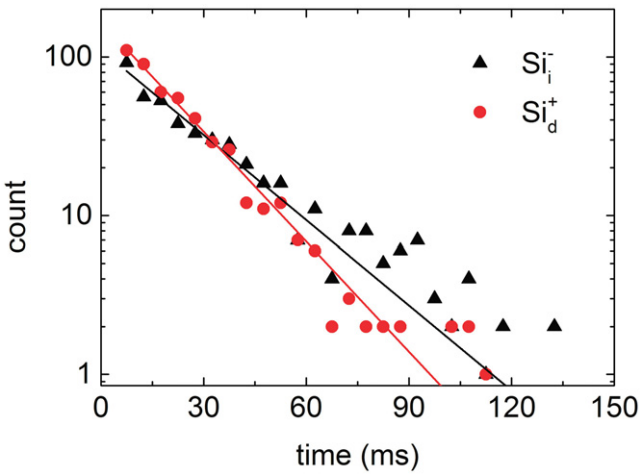

Figure 5. Residence time histograms of Si_i^- (red) and Si_d^+ (black) on a semi-logarithmic scale, $V = +0.98$ V, $I = 150$ pA, $T = 5$ K. Dots are the data and lines are the fits with equation (1).

cannot escape, because both the Fermi level of the tip and of the bulk sample are higher than the dopant level located ~500 meV below the conduction band edge [19, 20]. The TIBB at the semiconductor-vacuum interface is created by the electric field from the nearby STM tip. If the positive TIBB is increased by increasing the applied bias voltage, see (*b*), the electrons can tunnel into the conduction band and escape. The onset of this process occurs when the Si_i^- level aligns with the Fermi level of the bulk semiconductor. In the case of illumination, there is a secondary process that is responsible for the escape of electrons. The above-bandgap photons create electron-hole pairs when they are absorbed, see (*c*). The holes accumulate in the sample surface below the tip because of the positive TIBB there. They can recombine with the electrons bound to the Si, illustrated in (*d*), and in that way switch the dopant to the positive charge state. The dependence of the capture and escape processes on the TIBB and photogenerated holes allows the manipulation of the Si charge state with the STM tip and the laser.

The photon energy was varied from below- to above-bandgap excitation to study its effect on bistable Si atoms [10]. This is shown in the experiment presented in figure 8(*a*). For constant power, the photon energy was tuned between $U_p = 1.41$ and 1.59 eV. Below-bandgap excitation prevents the creation of electron-hole pairs, which limits the switching to Si_d^+. However, the broad energy tail extending from the bandgap energy $E_g = 1.52$ eV to lower energies is explained by the Franz–Keldysh effect, which promotes below-bandgap excitation in the presence of an electric field. Furthermore, a variation of the applied bias voltage reveals different regimes for the switching behavior. In (*b*), the results are shown of an experiment where the laser was turned on and off repetitively and the bias voltage was changed for every cycle. The positive charge state is favored at high bias voltage and thus the laser does not have an influence on the occupation. This is because the electrons escape through tunneling into the conduction band because of the high TIBB. For intermediate voltages, the situation of figure 6(*a*) is repeated. When the laser is off, Si_i^- is predominant, because the TIBB is too small to allow electrons to escape into the conduction band. In the case of illumination, holes are generated that can recombine with the electrons captured on the Si. For relatively low bias voltages, the Si is found stable in the positive charge state, regardless of the illumination on or off. In this case, the TIBB is so low that electrons do not have enough energy to overcome the energy

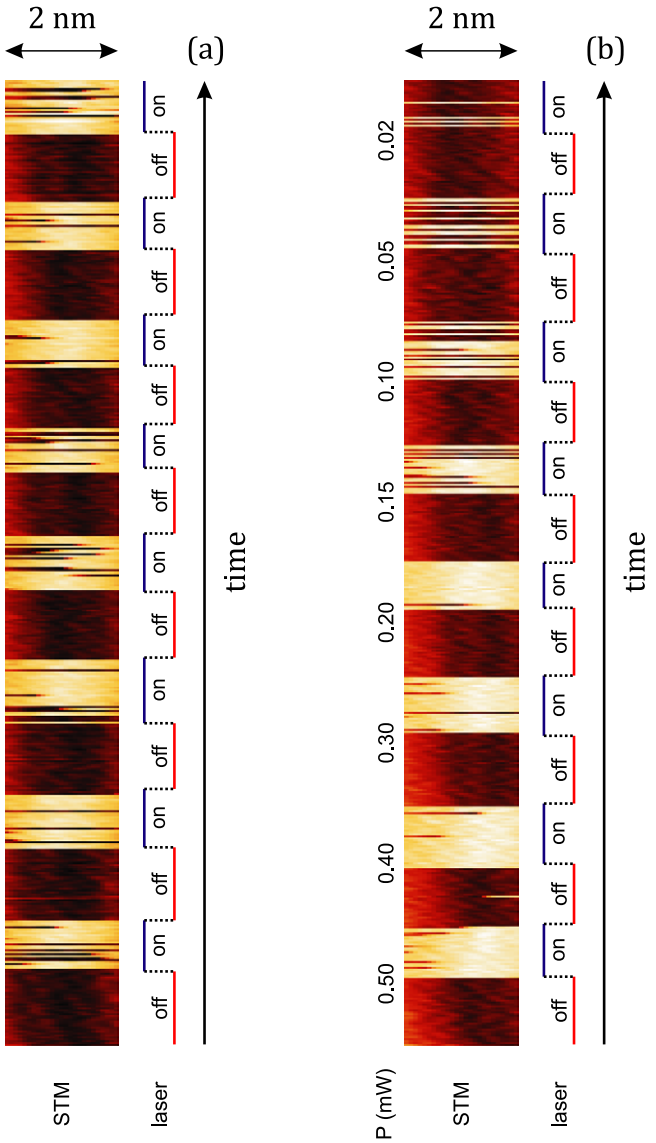

Figure 6. Twelve-minute-long line traces on top of a bistable Si. (*a*) Demonstration of the effect of illumination: the laser was repetitively turned on and off. (*b*) Similar experiment but in between each on-off cycle, the laser power was changed. $V = +0.50$ V, $I = 50$ pA, $T = 5$ K, $P = 0.25$ mW, $U_P = 1.96$ eV. Reproduced with permission from [10]. Copyright 2013 by the American Physical Society.

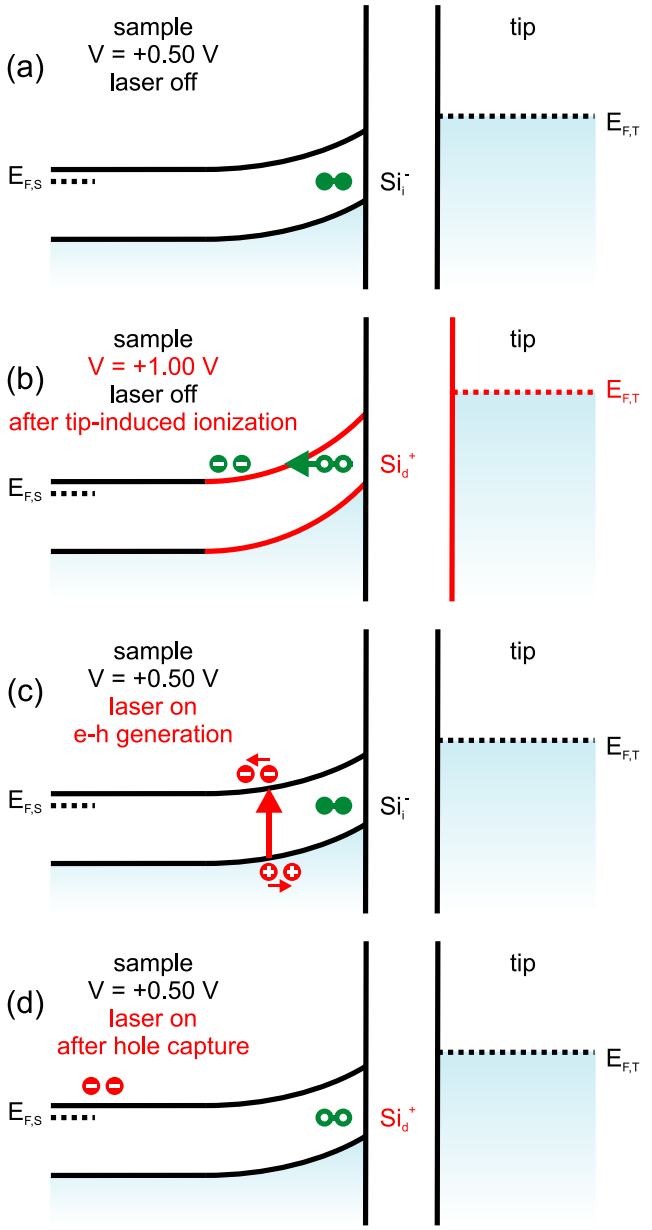

Figure 7. The relevant processes for the switching of the Si dopant explained in terms of energy diagrams of the tip-sample system. (*a*) The TIBB is relatively small, preventing the electrons from escaping into the conduction band, which favors Si_i^-. (*b*) A higher bias voltage induces ionization of the dopant, resulting in Si_d^+. (*c*) Under illumination, electron-hole pairs are created. The holes accumulate in the sample below the tip, close to the bistable Si atom. (*d*). The accumulated holes can recombine with the bound electrons on the negatively charged Si. This creates an alternative escape path for electrons, allowing the switch to Si_d^+. Reproduced with permission from [10]. Copyright 2013 by the American Physical Society.

barrier and allow the Si atom to switch between the positive and the negative charge configuration.

3. Dynamics

The switching dynamics of bistable Si atoms were studied in detail by analyzing the random telegraph noise signal of single dopants as a function of temperature, lateral distance between the tip and the dopant, bias voltage, and tunneling current.

The temperature dependence of the switching was investigated between $T = 5$ and 50 K, see figure 9. The switching frequency was extracted from complete 2D topographic images that were recorded for different temperatures at the same position. The switching frequency f of two single bistable Si dopants is depicted in black and red, (*a*) taken at $I = 25$ pA and (*b*) taken at $I = 250$ pA. In (*c*), the data for both current setpoints is combined. All datasets are fitted with an expression for a thermally excited process [15]:

$$f = \tau_0^{-1} + \nu \cdot \mathrm{e}^{-E_{\mathrm{bar}}/k_b T}, \qquad (2)$$

where ν is an amplitude for the thermal excitation, E_{bar} is the energy barrier, and τ_0^{-1} is a temperature-independent

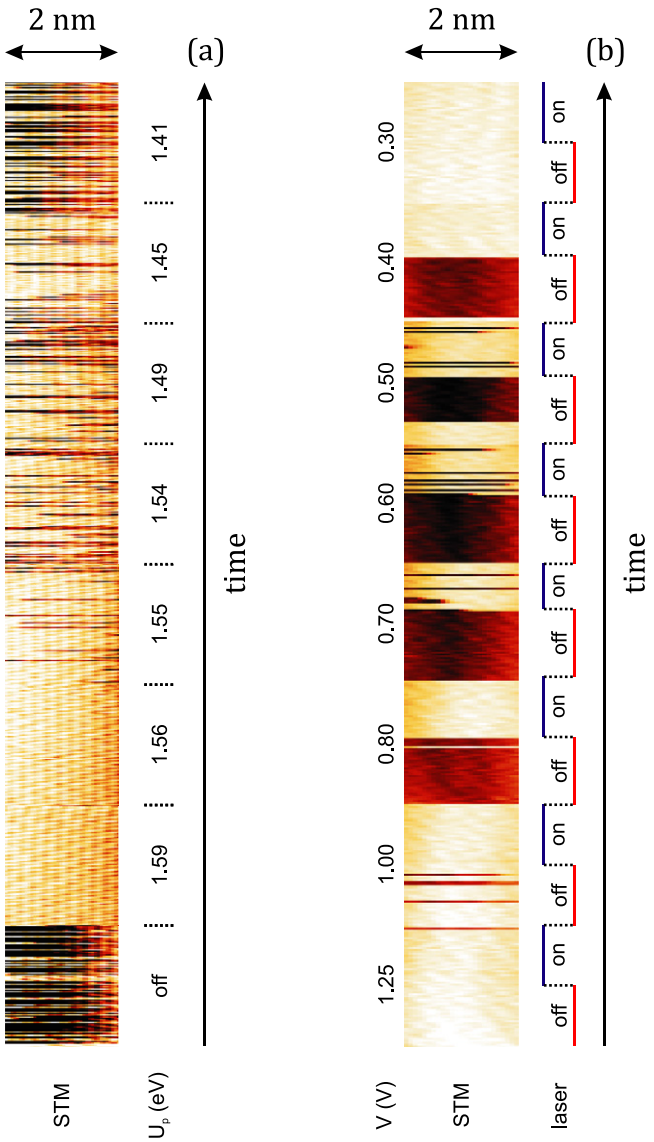

Figure 8. Twelve-minute-long line traces on top of a bistable Si, during which the laser was turned on and off repeatedly. (*a*) In between every on-off cycle, the photon energy was changed, $V = +0.65$ V, $I = 100$ pA, $P = 0.20$ mW. (*b*) The bias voltage was changed in between every on-off cycle, $I = 50$ pA, $P = 0.25$ mW, $U_p = 1.96$ eV. $T = 5$ K. Reprinted with permission from [10]. Copyright 2013 by the American Physical Society.

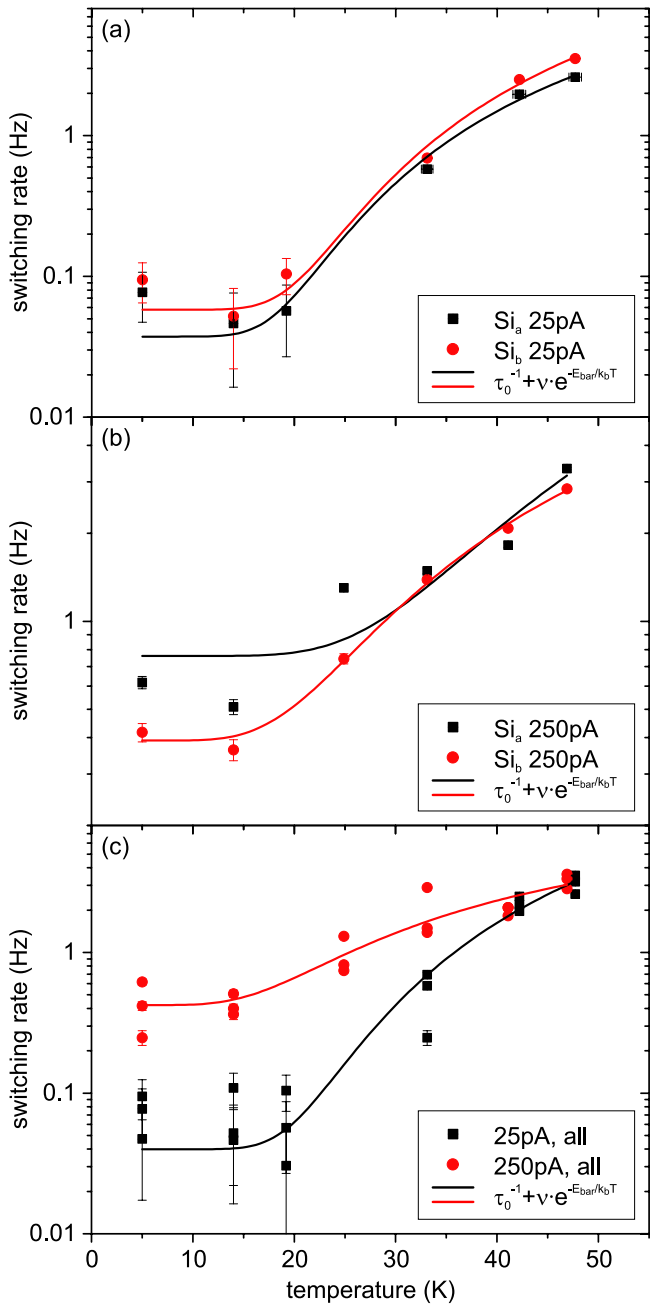

Figure 9. Temperature dependence of the switching frequency on semi-logarithmic scales, taken at (*a*) $I = 25$ pA, (*b*) $I = 250$ pA, and (*c*) for the data from both currents combined. $V = +1.00$ V. Dots are the data and lines are the fits with equation 2. Adapted with permission from [15]. Copyright 2011 by the American Physical Society.

frequency. The fits agree well with the data. For low temperature, a finite constant frequency $f = \tau_0^{-1}$ remains, which shows the importance of non-thermal contributions to the switching behavior. In these measurements, the non-thermal contributions are $\leqslant 1$ Hz. Furthermore, from the fits, a barrier height $E_{\mathrm{bar}} = 12 \pm 3$ meV was extracted, which is a measure for the energy needed to switch between the two charge configurations.

To study the low-temperature dynamics of a single bistable Si atom, or the τ_0^{-1} part of equation (2), switching frequency and charge state occupation maps were made of an 8×6 nm^2 area with the same 0.1 nm resolution as the STM topography recorded at $T = 5$ K, see figures 10(*a*) and (*b*). These maps were made by combining the STM with analog electronics that extract the frequency and charge occupations from the analysis of the topography, which is further described in [25] and [26]. Both the switching frequency and the charge state occupation are strongly dependent on the location of the STM tip. This is because the TIBB and the current density at the location of the dopant atom are different when the tip changes position. Therefore, the capture and escape processes of electrons are influenced by the exact location of the tip. With the tip on top of the Si atom, the TIBB is relatively high, favoring the escape of electrons and the occupation of Si_d^+. When the tip is a few nm away from the dopant atom, the TIBB at the position of the

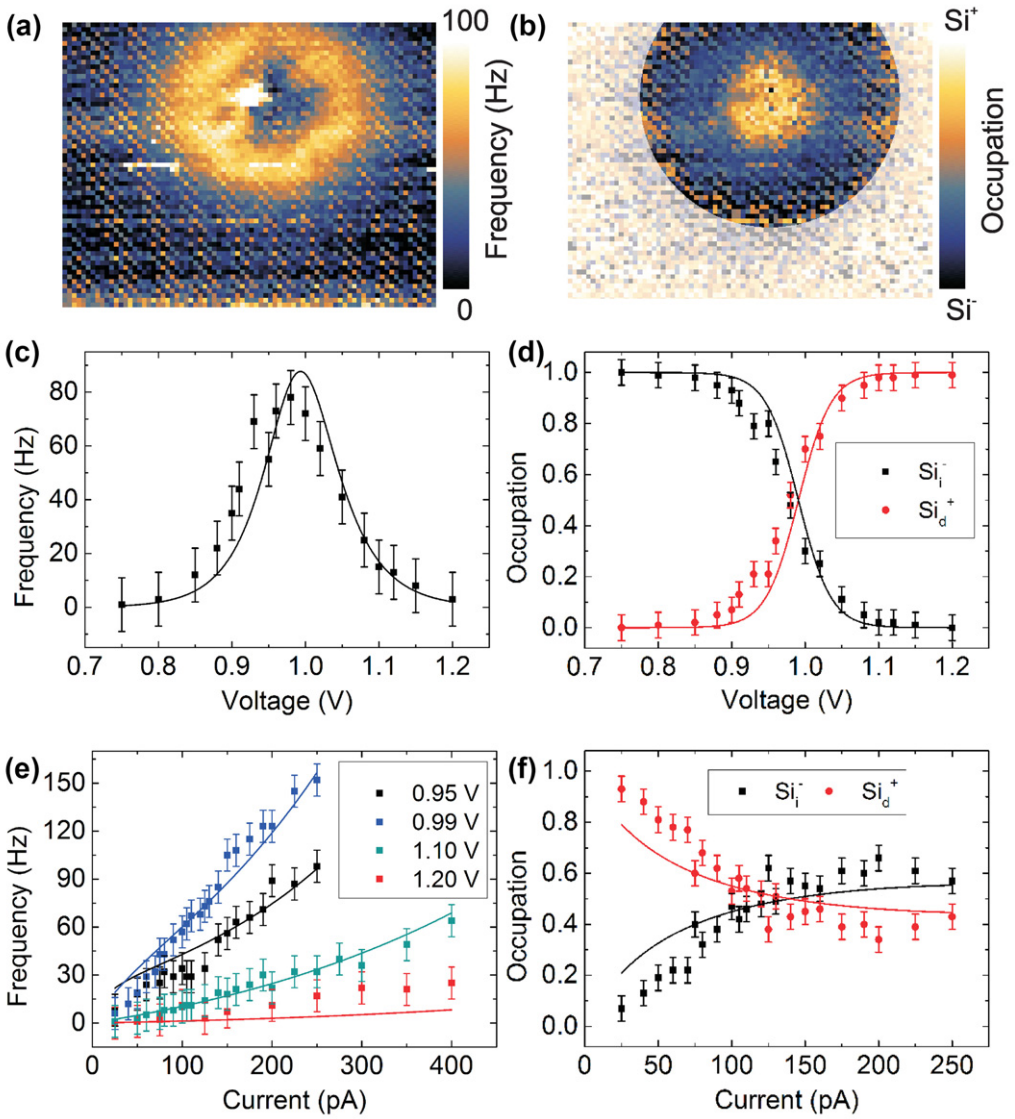

Figure 10. The dynamical behavior of single Si atoms. The lateral variation of (*a*) the switching frequency and (*b*) the charge state occupation for the same Si dopant. $8 \times 6\,\mathrm{nm}^2$, $V = +0.75\,\mathrm{V}$, $I = 500\,\mathrm{pA}$. In (*b*) the data is shown within a circle of confidence. (*c*)–(*f*) Switching frequency and charge state occupation as a function of bias voltage and tunneling current for the same Si dopant. (*c*) $I = 150\,\mathrm{pA}$, (*d*) $I = 150\,\mathrm{pA}$, (*f*) $V = +0.99\,\mathrm{V}$. Dots are the data and lines are the fits with equation (5). $T = 5\,\mathrm{K}$. Reprinted with permission from [16]. Copyright 2014 by the American Physical Society.

Si drops and the negative charge state is more easily occupied. At the same time, this results in a higher switching frequency. At even larger distances between the tip and the dopant, the electron escape process is very improbable, which favors the Si_i^- occupation and limits the switching to Si_d^+. Furthermore, the switching frequency and charge state occupation of a single Si atom were probed by restricting the STM tip to a position on top of the dopant and recording the height of the tip in time. The results are presented in (*c*)–(*f*). The switching occurs most often around a critical bias voltage, as shown in (*c*). This is also the situation where the positive and negative charge state both have an occupation of 0.50, visible in (*d*). This means that the probability of electron capture and escape is equal at the applied tunneling conditions. The results shown in (*e*) reveal that the switching rate scales roughly linearly with the tunneling current. Also, the occupation of the negative charge is favored more at higher currents, demonstrated in (*f*). This shows that the injection of more current by the STM tip drives the system towards more electron capture on the Si atom.

In figure 11, measurements on three different bistable Si are compared. The switching frequency data as function of bias voltage were obtained with different tips on similar samples. It is clear from the experiments that the maximum frequency is at a different bias voltage for each dopant and that the width of the distribution also changes. We expect that the electron capture and escape processes of a bistable Si depend strongly on the local electrostatic environment in the sample [27] and on the TIBB that, in turn, depends on the exact work function of the tip [28].

A bistable system can be described in terms of the average down time $\langle \tau_- \rangle$ and average up time $\langle \tau_+ \rangle$ [16]. A full switching cycle is the sum of these two. To model the switching dynamics of the bistable Si, the relevant tunneling barriers

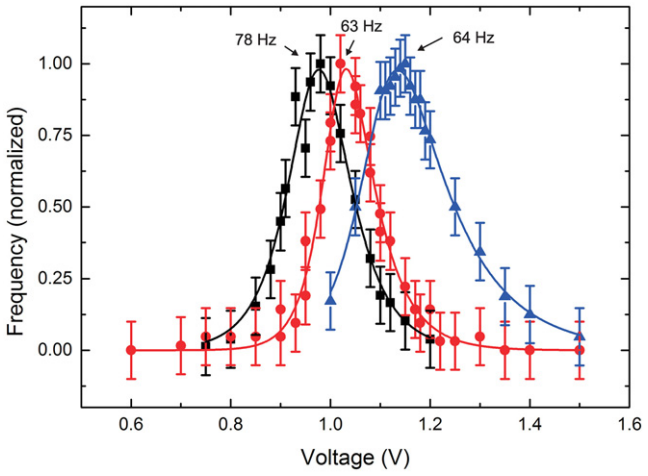

Figure 11. Comparison of the switching frequency dependence on applied bias voltage between three single bistable Si dopants. Measurements were taken with different tips at $I = 150\,\text{pA}$ (black), $I = 80\,\text{pA}$ (red), and $I = 95\,\text{pA}$ (blue). The data was normalized to the peak frequency, which is indicated for each curve. Dots are the data and lines are the fits with equation (5). $T = 5\,\text{K}$.

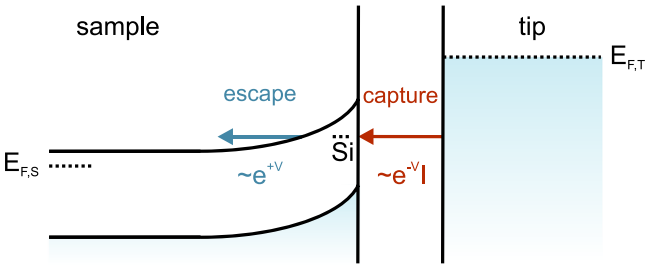

Figure 12. Illustration of the capture and escape processes on a bistable Si atom, with an STM tip in tunneling contact on top. Reprinted with permission from [16]. Copyright 2014 by the American Physical Society.

must be taken into account. The important physical processes are summarized in figure 12. The electron capture process is influenced by the vacuum barrier between the dopant and the tip. If the tip comes closer, the dopant level is more easily accessible for tunneling electrons. Therefore, the capture frequency $f_{+|-}$ increases with lower bias voltage and higher tunneling current. Additionally, $f_{+|-}$ is directly proportional to the amount of electrons that are injected and is thus is linear with the tunneling current. The parameters a_1, b_1, and c_1 are scaling constants:

$$f_{+|-} = \langle \tau_- \rangle^{-1} = a_1 \cdot \mathrm{e}^{-\frac{V}{b_1}+\frac{I}{c_1}} \cdot I. \tag{3}$$

The electron escape process depends on how easy it is to tunnel into the conduction band. The chance of tunneling or escape frequency $f_{-|+}$ increases when the TIBB increases because the barrier between the dopant level and the conduction band decreases. A higher TIBB is obtained with either increasing the bias voltage or the tunneling current. The parameters a_2, b_2, and c_2 are scaling constants:

$$f_{-|+} = \langle \tau_+ \rangle^{-1} = a_2 \cdot \mathrm{e}^{+\frac{V}{b_2}+\frac{I}{c_2}}. \tag{4}$$

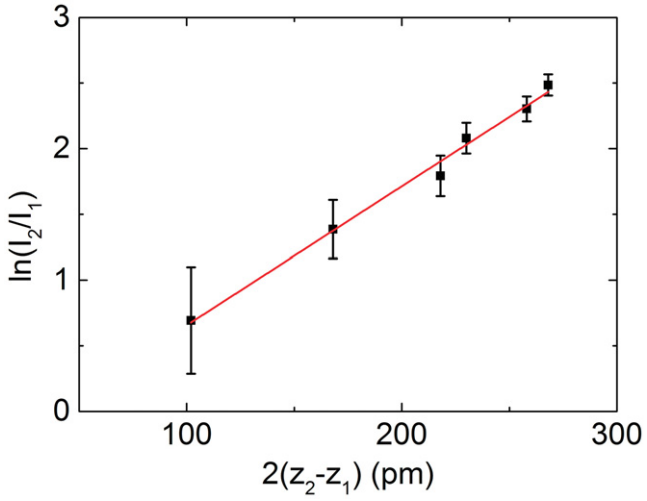

Figure 13. Logarithmic current ratio as a function of tip height difference, taken from the data shown in figures 10(*c*)–(*f*), which allows the extraction of the decay length κ. Black dots are the data and the red line is a linear fit using equation (6).

The total switching frequency f, the negative charge state occupation n_-, and the positive charge state occupation n_+ are:

$$\begin{aligned} f = \langle \tau \rangle^{-1} &= \frac{f_{+|-} \cdot f_{-|+}}{f_{+|-} + f_{-|+}}, \\ n_- &= f_{-|+}^{-1} \cdot f, \\ n_+ &= f_{+|-}^{-1} \cdot f. \end{aligned} \tag{5}$$

The fits with equation (5) agree well with the data displayed in figures 10(*c*)–(*f*). For the complete dataset of four different graphs, we used the following universal fitting parameters: $a_1 = 1.3\,\text{GHz}\,\text{pA}^{-1}$, $a_2 = 4.7\,\mu\text{Hz}$, $b_1 = 47\,\text{mV}$, $b_2 = 42\,\text{mV}$, $c_1 = 0.60\,\text{nA}$ and $c_2 = 0.20\,\text{nA}$. The model accurately describes the quantum tunneling processes involved in the switching of the bistable Si dopants when the STM tip is near.

We estimate the effect of TIBB for the data shown in figures 10(*c*)–(*f*) by determining the band bending at the surface from $I(Z)$ data [28, 29]. The exponential relation between tunneling current I and tip-sample distance d depends on the decay length κ [30]:

$$I \propto \exp(-2\kappa d). \tag{6}$$

By measuring the topographic height for various setpoint currents, we can extract κ. In figure 13, the logarithmic current ratio between two tunneling conditions is displayed against the tip height difference for the same two settings. The slope of the linear fit yields a decay length of $\kappa = 10.6 \pm 0.5\,\text{nm}^{-1}$. This quantity is converted to an effective barrier height Φ_B by:

$$\Phi_\text{B} = \frac{\kappa^2 \hbar^2}{2m_0}, \tag{7}$$

where $\hbar$ is the reduced Planck's constant and m_0 i the electron rest mass. This gives $\Phi_\text{B} = 4.3 \pm 0.4\,\text{eV}$. By using the calculation model from [31], which solves the

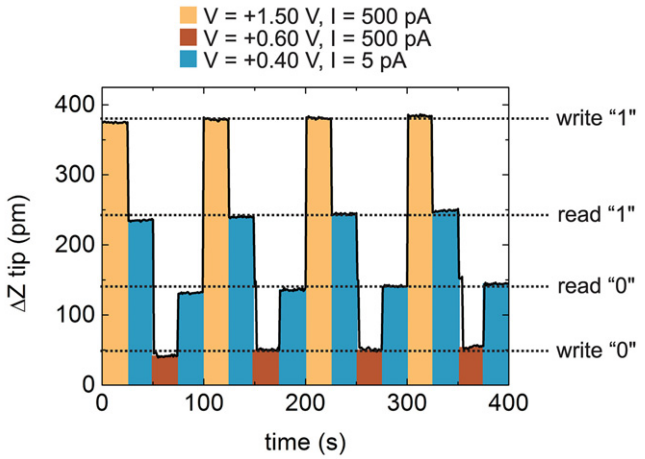

Figure 14. Repeated memory operations on a single bistable Si atom, with the tip acting as a gate. Si_i^- is state (0) and Si_d^+ is state (1). $T = 5$ K. Reprinted with permission from [16]. Copyright 2014 by the American Physical Society.

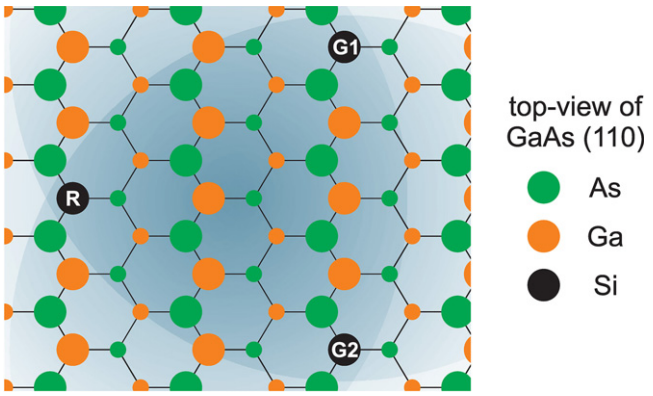

Figure 15. Visualization of three bistable Si in the GaAs surface used as a logic gate, where the disks around the dopants indicate the Coulomb effect they exert on their surroundings. The two gates $G1$ and $G2$ are manipulated by a scanning probe method and result in setting the result dopant R. This configuration would allow, for example, NAND or NOR operation, depending on the distance of the dopants to each other.

Poisson equation iteratively, the flatband condition V_{FB} can be determined, which is the applied bias voltage at which there is no band bending at the semiconductor surface. Additionally, from this information, the band bending energy at the surface E_{BB} can be calculated for every applied bias voltage. We obtain $V_{FB} = -0.9 \pm 0.7$ V. The switching frequency has a maximum at $V = +0.98$ V, which results in a TIBB of $E_{BB} = 0.4 \pm 0.2$ eV. These values demonstrate that there is positive band bending for all applied tunneling conditions, as assumed in the analysis of this work. Furthermore, because we observe that the switching process begins roughly above $V = +0.80$ V, the corresponding TIBB of $E_{BB} = 0.3 \pm 0.1$ eV is an estimate of the binding energy of the Si_i^- state. This corresponds to DFT calculations that predict this state is located much deeper in the bandgap than the donor state [19, 20].

The bistable Si atom in the GaAs (1 1 0) surface provides a system for storing information. For operating any system as a memory cell, two distinct states should be available that can reproducibly be written and read out. The bistable Si atom was employed as a memory element with the STM tip acting as a gate [16]. The experimental data is presented in figure 14, where the charge state was set and detected repetitively using three different tunneling conditions: (a) a relatively high voltage to write the Si into Si_d^+, (b) an intermediate voltage to write Si_i^-, and (c) a relatively low voltage to read out the charge state without affecting it. The low tunneling current used in the read out condition was applied for more stability. The experiment was repeated four times to demonstrate the reproducibility of the system. At the experimental temperature of $T = 5$ K, the charge state remained stable during all applied tunneling conditions.

Multiple bistable Si atoms in the surface can interact with each other if they are close. In principle, this might be used to create logical devices if the position of the dopants can be controlled precisely, for example, by employing STM [32, 33] or atomic force microscopy (AFM) [3, 34].

In figure 15, a visualization is depicted of three bistable Si that influence each other through Coulomb effects, allowing the construction of logic operators. If the Si are relatively far from each other, for example, two input (1) states are needed to switch the output to (0), which effectively results in a NAND gate. Putting them closer together would then result in a NOR gate, because then only a change in one input is needed to switch the output state.

4. Conclusion

In this work, recent investigations with STM on bistable Si atoms in the GaAs (1 1 0) surface layer are reviewed. The switching of the Si dopants is manipulated by tuning the local band bending with the STM tip and by illuminating the sample with a laser. Both the thermal and quantum tunneling contributions to the switching behavior are described with a physical model, which agrees with experimental observations. Furthermore, a bistable Si atom was employed as a memory element, where writing and reading of information was achieved by using the STM tip as a gate.

Acknowledgment

The funding for this work was provided by FOM (Grant 09NSE06).

References

[1] Moore G E 1965 *Electronics* **38** 114
[2] Koenraad P M and Flatté M E 2011 *Nat. Mater.* **10** 91
[3] Repp J, Meyer G, Olsson F E and Persson M 2004 *Science* **305** 493
[4] Yang J, Erwin S C, Kanisawa K, Nacci C and Fölsch S 2011 *Nano Lett.* **11** 2486
[5] Haider M B, Pitters J L, DiLabio G A, Livadaru L, Mutus J Y and Wolkow R A 2009 *Phys. Rev. Lett.* **102** 046805
[6] Schofield S R, Studer P, Hirjibehedin C F, Curson N J, Aeppli G and Bowler D R 2012 *Nat. Commun.* **4** 1649
[7] Fuechsle M, Miwa J, Mahapatra S, Ryu H, Lee S, Warschkow O, Hollenberg L C L, Klimeck G and Simmons M Y 2012 *Nat. Nanotechnol.* **7** 242

[8] Zheng H, Weismann A and Berndt R 2014 *Nat. Commun.* **5** 2992
[9] Garleff J K, Wenderoth M, Sauthoff K, Ulbrich R G and Rohlfing M 2004 *Phys. Rev.* B **70** 245424
[10] Smakman E P, Van Bree J and Koenraad P M 2013 *Phys. Rev.* B **87** 085414
[11] Zheng J F, Liu X, Newman N, Weber E R, Ogletree D F and Salmeron M 1994 *Phys. Rev. Lett.* **72** 1490
[12] Feenstra R M, Meyer G, Moresco F and Rieder K H 2002 *Phys. Rev.* B **66** 165204
[13] Domke C, Ebert P and Urban K 1998 *Surf. Sci.* **415** 285
[14] Loth S, Wenderoth M, Teichmann K and Ulbrich R G 2008 *Solid State Commun.* **145** 551
[15] Garleff J K, Wijnheijmer A P, Van Den Enden C N and Koenraad P M 2011 *Phys. Rev.* B **84** 075459
[16] Smakman E P, Helgers P L J, Möller V J R and Koenraad P M 2014 *Phys. Rev.* B **90** 041410(R)
[17] Teichmann K, Wenderoth M, Loth S, Ulbrich R G, Garleff J K, Wijnheijmer A P and Koenraad P M 2008 *Phys. Rev. Lett.* **101** 076103
[18] Wijnheijmer A P, Garleff J K, Teichmann K, Wenderoth M, Loth S and Koenraad P M 2011 *Phys. Rev.* B **84** 125310
[19] Wang J, Arias T A, Joannopoulos J D, Turner G W and Alerhand O L 1993 *Phys. Rev.* B **47** 10326
[20] Yi Z, Ma Y and Rohlfing M 2011 *J. Phys. Chem.* C **115** 23455
[21] Chadi D J and Chang K J 1989 *Phys. Rev.* B **39** 10063
[22] Mooney P M 1991 *Semicond. Sci. Technol.* **6** B1
[23] Van Houselt A and Zandvliet H J W 2010 *Rev. Mod. Phys.* **82** 1593
[24] Keizer J G, Garleff J K and Koenraad P M 2009 *Rev. Sci. Instrum.* **80** 123704
[25] Schaffert J, Cottin M C, Sonntag A, Karacuban H, Bobisch C A, Lorente N, Gauyacq J-P and Möller R 2013 *Nat. Mater.* **12** 223
[26] Schaffert J, Cottin M C, Sonntag A, Karacuban H, Utzat D, Bobisch C A and Möller R 2013 *Rev. Sci. Instrum.* **84** 043702
[27] Teichmann K, Wenderoth M, Loth S, Garleff J K, Wijnheijmer A P, Koenraad P M and Ulbrich R G 2011 *Nano Lett.* **11** 3538
[28] Wijnheijmer A P, Garleff J K, Van Der Heijden M A and Koenraad P M 2010 *J. Vac. Sci. Technol.* B **28** 1086
[29] Loth S, Wenderoth M, Ulbrich R G, Malzer S and Döhler G H 2007 *Phys. Rev.* B **76** 235318
[30] Chen C 1993 *Introduction to Scanning Tunneling Microscopy* (Oxford: Oxford University Press)
[31] Feenstra R M 2003 *J. Vac. Sci. Technol.* B **21** 2080
[32] Kitchen D, Richardella A, Tang J-M, Flatté M E and Yazdani A 2006 *Nature* **442** 436
[33] Lee D H and Gupta J A 2011 *Nano Lett.* **11** 2004
[34] Gross L, Mohn F, Liljeroth P, Repp J, Giessibl F J and Meyer G 2009 *Science* **324** 1428